

ON THE EVOLUTION OF ACCRETION RATES IN COMPACT OUTBURST SOURCES

SAMIR MANDAL^{1,2} AND SANDIP K. CHAKRABARTI^{1,3}

¹ Indian Centre for Space Physics, Chalantika 43, Garia Station Rd., Kolkata 700084, India; samir@csp.res.in

² Department of Physics, Ben-Gurion University of the Negev P.O. Box 653, Beer-Sheva 84105, Israel

³ S.N. Bose National Centre for Basic Sciences, JD Block, Salt Lake, Sector III, Kolkata 700098, India; chakraba@bose.res.in

Received 2009 October 2; accepted 2010 January 19; published 2010 February 3

ABSTRACT

Spectra in outburst sources are found to become soft in viscous timescales before going back to hard as in the pre-outburst phase. By using two component accretion disks we show that major characteristics of the spectral evolution can be reproduced. We find that the outburst is possibly caused by a sudden rise in viscosity which gradually converts the sub-Keplerian flow into a Keplerian flow. The decline of the viscosity reduces the Keplerian accretion rate, and the system goes back to hard states. We discuss the genesis of the characteristic shape of the hardness–intensity diagram and reproduce this for the well-known outburst source GRO J1655-40.

Key words: accretion, accretion disks – black hole physics – hydrodynamics – shock waves – stars: neutron

1. INTRODUCTION

Compact objects such as black holes and neutron stars show considerable variation in photon intensities and spectral behavior. This is true even for massive and supermassive black holes which belong to galactic nuclei. The cause is generally understood to be due to the variation of the rate of matter accreting onto the compact object. In the standard Shakura–Sunyaev model (Shakura & Sunyaev 1973, hereafter SS73), a single accretion rate along with viscous parameter α determines the nature of the intensity variation while in more advanced models such as in Chakrabarti & Titarchuk (1995, hereafter CT95), two accretion rates, one for the Keplerian flows and the other for the sub-Keplerian flows, are employed instead. Subsequently, it was shown by Chakrabarti (1997, hereafter C97), Chakrabarti & Mandal (2006, hereafter CM06), Mandal & Chakrabarti (2008), and Chakrabarti et al. (2008, 2009) that two rates are necessary and sufficient to describe the varied spectral and timing properties of all types of black hole candidates. The presence of two accretion rates has been pointed out by others while interpreting observational results from black holes (Soria et al. 2001; Wu et al. 2002; Smith et al. 2001, 2002; Choudhury & Rao 2004; Pottschmidt et al. 2006; Smith et al. 2007). Variation of these two rates would yield varied spectral states, and very often we can get important information about the accretion processes by fitting data at various stages of evolution, especially in outburst sources.

In this Letter, we propose an explanation of the evolutions of outburst sources and fit the spectra with two component flows. We show that, typically, the sources start with very low Keplerian accretion rates and a large sub-Keplerian accretion rate. When there is a surge in viscosity, the sub-Keplerian matter is converted to the Keplerian matter due to the transport of angular momentum, and the Keplerian matter slowly moves in closer to a black hole in the viscous timescale. This was shown before by numerical simulations (Chakrabarti & Molteni 1995). As the Keplerian accretion rate is enhanced, the spectrum becomes softer. When the viscosity decreases, the decline phase of the outburst starts, and the Keplerian region recedes back and the hard state is regained. Though generally this picture has been around for a long time (Chakrabarti 1997), no quantitative study has been made to actually show that this is indeed the

case. In the next Section, we present our model. In Section 3, we generate the so-called hardness–intensity diagram (HID) ab initio by an assumed but realistic variation of the accretion rates in the Keplerian and sub-Keplerian components. In Section 4, we compare our solution with observations for the well-known black hole candidate GRO 1955-40 as an example. Finally, in Section 5, we make concluding remarks.

2. MODEL DESCRIPTION

We consider a two-component advective disk model (CT95) around a black hole. The viscous Keplerian disk located on the equatorial plane is sandwiched by a low angular momentum and weakly viscous sub-Keplerian flow. The sub-Keplerian flow can have a centrifugal pressure supported standing or moving shock wave depending on the initial energy and angular momentum of the flow. As in any compact star, this post-shock region behaves as a boundary layer of a black hole. Particularly, for black holes, this is the source of hot electrons which Comptonize the soft photons from the Keplerian disk. This region is termed a CENBOL (CENTrifugal pressure supported BOUNDary Layer).

In our computation of the spectrum arising out of the composite disk, we use the radial distance (x) in units of the Schwarzschild radius ($r_g = 2GM/c^2$), where G is the gravitational constant, M is the mass of the black hole, and c is the speed of light. The parameters of our model are: the shock location (x_s) and the accretion rates of the Keplerian (\dot{m}_d) and the sub-Keplerian halo (\dot{m}_h) components. The accretion rates are measured in units of the Eddington rate ($\sim 0.2 \times 10^{-7} M_\odot/\text{yr}$ for a $10 M_\odot$ black hole). For simplicity, we use the compression ratio (R) of the shock as $R = 4$. We have fixed the outer boundary of the accretion disk at $x = 10^6$, and the injection temperature for electrons and protons in the sub-Keplerian flow was chosen to be $T_e = T_p = 1.6 \times 10^6$ K. We verified that the result is not sensitive to the choice at the outer boundary. For details of our model, see Mandal & Chakrabarti (2008) and references therein. The formation of a hysteresis-like loop in the HID is primarily due to the multiple-valued nature of the spectral index. As shown in CT95 (see, Figure 3(a)) and C97, this is possible if there are two components. A loop is formed when their variations have two different timescales.

3. GENERATION OF HARDNESS–INTENSITY DIAGRAMS

Several outburst sources (such as GRO J1655-40 and XTE J1550-564) have been extensively studied recently (Rodriguez et al. 2003; Shaposhnikov et al. 2007; Debnath et al. 2008; Corbel et al. 2006). It is generally agreed that the outburst is due to a sudden change in the boundary condition of the accretion disk. In a two-component flow, a perturbation in the sub-Keplerian component propagates in the infall timescale whereas that in the Keplerian component propagates in the viscous timescale ($t_v = r^2/(\alpha h a_s)$, with r being the radial distance, α being the Shakura–Sunyaev [SS73] viscosity parameter, $h = h(r)$ being the disk thickness, and $a_s = a_s(r)$ being the speed of sound). We assume that in the quiescence state the accreting matter is generally sub-Keplerian in nature and the outburst is triggered because of a sudden change in the viscosity of the flow at the outer boundary which leads to the conversion of the sub-Keplerian matter into the Keplerian matter (C97), keeping the total mass accretion rate ($\dot{m}_d + \dot{m}_h$) nearly constant. In our model, the outburst is mainly controlled by three time-varying parameters: namely, \dot{m}_d , \dot{m}_h , and x_s . From the nature of the typical outbursts, it appears that in a complete burst episode, a total of four timescales are important, one for the rising phase (t_r) and the other three (t_d , t_h , and t_s) for the declining phases of the three independent parameters (\dot{m}_d , \dot{m}_h , and x_s), respectively.

A sufficiently general behavior of the time-dependent accretion rates and the shock locations is as follows. Here, the rates are in units of the Eddington rate and time is in units of days. The Keplerian accretion rate varies as

$$\dot{m}_d = \begin{cases} A_f [(t_r + 1) - t]^{\alpha_d}, & t < t_r \\ A_f, & t_r \leq t < t_d \\ A_f [t - (t_d - 1)]^{\alpha_d}, & t \geq t_d. \end{cases} \quad (1)$$

The sub-Keplerian accretion rate varies as

$$\dot{m}_h = \begin{cases} B_f, & t < t_r \\ B_f [(t - (t_r - 1))^{\alpha_{h1}}], & t_r \leq t < t_h \\ B_f [(t_h - (t_r - 1))^{\alpha_{h1}} [t - (t_h - 1)]^{\alpha_{h2}}], & t_h \leq t < t_s \\ B_f, & t \geq t_s. \end{cases} \quad (2)$$

The shock location varies as

$$x_s = \begin{cases} X_{S_o} - v_0 t, & t < t_r \\ X_{S_i}, & t_r \leq t < t_s \\ X_{S_i} + v_0 (t - t_s), & t \geq t_s. \end{cases} \quad (3)$$

All of the 12 parameters, namely, A_f , B_f , t_d , t_r , t_h , t_s , α_d , α_{h1} , α_{h2} , X_{S_o} , X_{S_i} , and v_0 are not independent, however. The constraint that \dot{m}_d arises out of \dot{m}_h gives rise to the maximum Keplerian accretion rate at $t = t_h$: $A_f = B_f [1 - (t_h - t_r + 1)^{\alpha_{h1}}]$. At $t = t_s$, the constraint on \dot{m}_h returning back to B_f gives $\alpha_{h2} = -\alpha_{h1} \ln(t_h - t_r + 1) / \ln(t_s - t_h + 1)$. In the decline phase, the disk is refilled by the sub-Keplerian matter (Equation (2)) in the time interval ($Dt = t_s - t_h$) which is basically the infall timescale of sub-Keplerian matter from the outer boundary, ~ 0.75 days in our case. Earlier evidence (Chakrabarti et al. 2008, 2009) of the shock velocity of a few tens of meters s^{-1} suggests $v_0 \sim 50 - 100 r_g/\text{day}$. This is related to X_{S_o} , since, $X_{S_o}/v_0 \sim t_r$. The same rise time must arise out of viscosity.

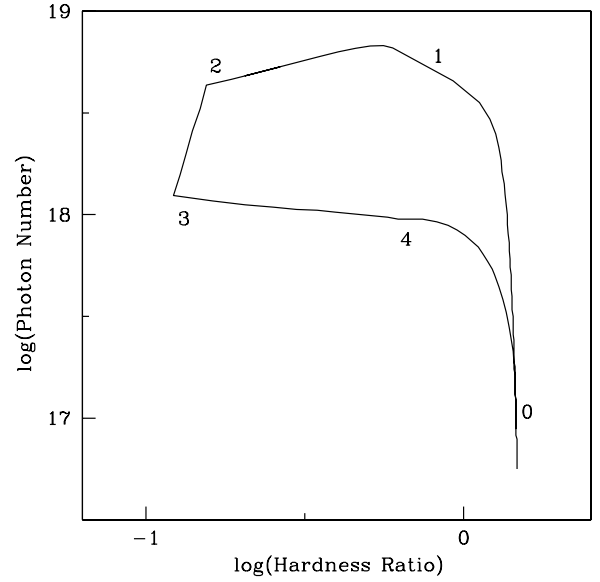


Figure 1. Example of the hardness ratio–photon intensity diagram for black holes. The description of different regions is given in the text.

Table 1
Input Parameters

Time (day)				α_d	α_{h1}	X_{S_o}	X_{S_i}	v_0	B_f
t_r	t_d	t_h	t_s			(r_g)	(r_g)	(r_g/day)	
12.0	12.5	12.75	14.3	-2.8	-4.2	730.0	10.0	60.0	3.5

Equating t_r with the viscous time-scale using an α parameter (e.g., $t_r \sim t_v \sim 12d$ for $\alpha = 0.03$) one obtains X_{S_o} . The timescale $t_d - t_r$ for which the Keplerian rate remains high is the duration of the high-viscosity regime (say, the washout time of strongly entangled magnetic field, when magnetic viscosity is important) and could be of the order of the free fall timescale Dt or more. Thus, the timescale $t_s \gtrsim t_r + 2 \times Dt$, when the shock recedes back to outer edge. In addition, to fit any spectrum at a given time we require three parameters (CT95, C97), say, \dot{m}_d , \dot{m}_h , and X_{S_i} . Thus, ultimately there are only two extra parameters, namely, α_d and α_{h1} . However, they are not arbitrary: our fits for various objects indicate $\alpha_d \sim -3$, $\alpha_{h1} \sim -4$, though the exact numbers will vary from outburst to outburst.

Our goal in this Letter is to see if by a choice of the suitable values of the time intervals which are specific to an outburst and a black hole, one could describe an outburst event. Though we can have the complete spectral evolution from these parameters, a simpler process could be to concentrate only on the color–color diagram or HID. Since the latter is used in the literature more often, we reproduce this diagram to get a general feeling of how the accretion rates and the shock location might be changing during a complete outburst process.

In Figure 1, we present an example of the hardness versus photon intensity diagram and mark the boundaries of the timescales by 0 to 4. For the sake of completeness and simplicity, we use the same set of parameters (Table 1) that we use to model the outburst source GRO J1655-40 (Figure 2). In the rising phase (0 to 1), the time t_r is taken by the Keplerian flow to reach the maximum accretion rate (A_f) and it remains there for $t_d - t_r$ (1–2). After that it starts to decrease monotonically (2 to 0). Following earlier evidence that the shock moves with a constant

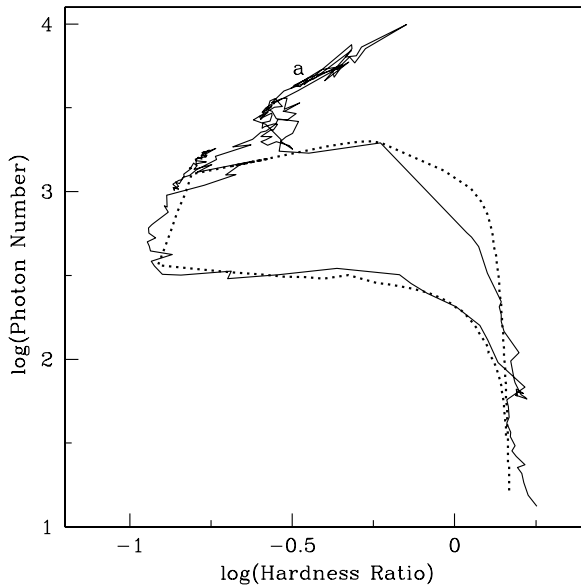


Figure 2. Fit of the GRO J1655-40 during its outburst (solid line) of 2005 with the model (dotted line). The parameters are given in Table 1.

velocity of a few tens of meters s^{-1} (Chakrabarti et al. 2008, 2009) we also assume a constant velocity (v_0) for the shock to move from the outer part of the disk (X_{s_o}) to the inner part (X_{s_i}) in time (0 to 1) in the rising phase. The shock stays there until the t_s (4) and then it starts to recede (4 to 0) in the decline phase. The sub-Keplerian accretion rate is assumed to be constant (B_f) for a period of t_r (0 to 1). It is drained between 1 and 3 in time $t_h - t_r$ and again increased during an interval of $Dt \sim t_s - t_h$. At $t = t_s$, the sub-Keplerian accretion rate returns back to its value near the pre-outburst phase and stays that way (regions 4 to 0). The timescales can be computed from average viscosity parameters, but we chose not to introduce new parameters due to poor knowledge of viscosity. While plotting, we calculated the spectrum and made a total photon count in the (3–20) keV band. The hardness ratio is the ratio between the number of photons in (6–20) keV and the number of photons in (3–6) keV. As shown in C97, the general effects of the three main parameters are found to be the following. (1) An increase in Keplerian accretion rate increases the photon counts and softens the spectrum. (2) An increase in the sub-Keplerian accretion rate increases the supply of hot electrons. So, the spectrum is hardened. (3) The inward movement of the shock increases the number of soft photons as the Keplerian disk also moves inward. This also softens the spectrum. This is observed near mark 1 in Figure 1 when the spectrum softens because of the inward movement of the shock.

At the onset of the outburst, a change in viscosity causes slow conversion of a sub-Keplerian flow into a Keplerian flow (C97). However, the soft photons are insufficient to cool a huge amount of sub-Keplerian flow $\dot{m}_h \sim B_f$. So the spectrum remains hard with almost constant spectral index (see, Figure 3(a) of CT95 for low \dot{m}_d) and thus, the hardness ratio remains almost constant. This continues till \dot{m}_d becomes high at the cost of \dot{m}_h . The total time taken for the Keplerian disk is the rise time of $t_r \sim t_v$. The shock also moves in as is evidenced by the gradual rise of the quasi-periodic oscillation (QPO) frequency, which, according to some models (Chakrabarti et al. 2008, 2009) is the inverse of the infall time in the post-shock region. A nearly constant photon count between 1 and 2 is maintained due to a constant Keplerian accretion rate and shock location. Subsequently, as the sub-Keplerian accretion rate decreases, the

spectrum is softened further since the hot electrons are rapidly cooled. Also, in this region of the diagram, high-frequency QPOs are observed. This could be because when the CENBOL is cooler, the only important length scales are the inner sonic point and the inner edge of the Keplerian disk whose oscillations are important. At 2, after the “cause of viscosity” is stopped, the Keplerian accretion rate starts to decrease causing a sharp jump (2 to 3) in photon counts. It continues till the black hole enters in the low/hard state. At 3, most of the sub-Keplerian matter is drained and the disk starts to refill between 3 and 4 in its infall timescale (< 1 day). This refilling of sub-Keplerian matter increases the hardness while keeping the photon counts almost constant. After point 4, the thermal pressure of the hot CENBOL pushes the shock outward, which decreases the photon counts even further which makes the spectrum harder. The important point to note is that the shape of the diagram near region 2 is very much sensitive to the time variation of the parameters. This is especially true because the number of soft photons is very high in comparison with the hot electrons (very soft state) and everything is happening very close ($5-10r_g$) to the black hole. That is why the observed HIDs are generally not of any regular shape in most of the cases and show considerable fluctuations.

4. A COMPARISON WITH OBSERVATION

The galactic black hole candidate GRO J1655-40 is a low mass X-ray binary with a primary mass $M = (7.02 \pm 0.22) M_\odot$ (Orosz & Bailyn 1997) and the companion star mass $= 2.3 M_\odot$, located at a distance of $D = (3.2 \pm 0.2)$ kpc (Hjellming & Rupen 1995). In Figure 2, we plot the hardness ratio versus photon intensity diagram of the observational data (e.g., Debnath et al. 2008) of GRO J1655-40 during its outburst of 2005 by the solid line. Here, we have plotted the total photon counts (3–20 keV) along the y-axis and the hardness ratio (ratio of photons in the 6–20 keV range and in the 3–6 keV range) along the x-axis. We plot the theoretically obtained curve by the dotted line. The average nature of the plot agrees well with the observation except in the very soft state (point *a* in Figure 2). This is understandable since in the very soft state when the two rates are comparable, the spectral index is very sensitive to the flow parameters (see, Figure 3(a) of CT95 near $\dot{m}_d \sim 1 - 3$). So, any small local perturbation can change the nature of the spectrum drastically. The parameters for this plot are given in Table 1. Note that the timescales in the rising phase ($t_r \sim 12$ days) and in the decline phase are consistent with that found (Chakrabarti et al. 2008) by fitting the evolution of QPO frequency and they are comparable to the viscous timescale. The time interval ($t_h - t_r \sim 0.75$ days), during which the sub-Keplerian matter is draining, is comparable to the free fall timescale for an accretion disk having outer boundary at $\sim 10^6 r_g$. Similarly, we chose $v_0 = 60r_g/\text{day}$, which corresponds to about 15 m s^{-1} . A choice of $v_0 \sim 82r_g/\text{d}$ (i.e., 20 m s^{-1}) and $X_{s_o} \sim 1000$ would also produce a similar result (Chakrabarti et al. 2008, 2009). In Figure 3, we plot the evolution of the accretion rates and the shock location during the outburst. The dotted curve and the dashed curve are the accretion rates of the disk and the halo, respectively. The solid curve is the variation of the shock location (in units of $100 r_g$ to plot in the same diagram). The four tick marks at t_r , t_d , t_h , and t_s are located at $t = 12, 12.5, 12.75,$ and 14.3 , respectively. We have chosen a conical geometry for the sub-Keplerian flow (Chakrabarti & Mandal 2006). The accretion rates will be scaled when the wedge angle of the flow is varied, but the general behavior of the variation of the accretion rate will remain the same. We did

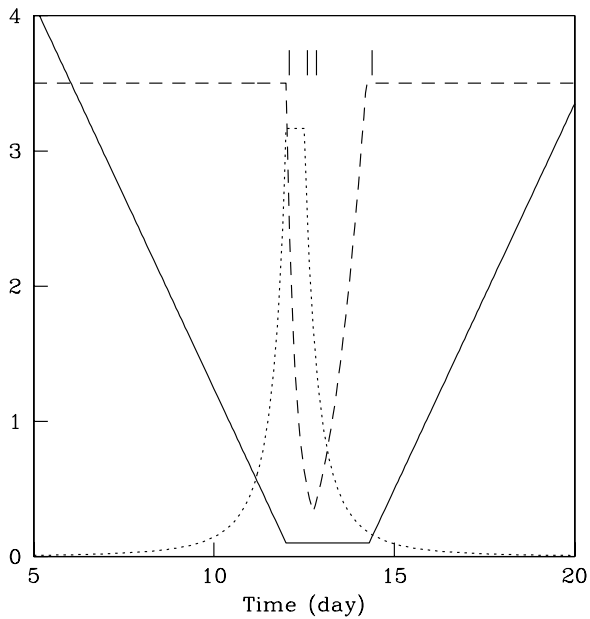


Figure 3. Variation of the disk rate (dotted), halo rate (dashed), and the shock location (solid). The rates are in units of the Eddington rate and the shock location is in units of $\sim 100r_g$. Note the reduction of the sub-Keplerian halo rate when the Keplerian accretion rate went up. This may be caused by a sudden rise in viscosity. Four vertical marks are at t_r , t_d , t_h , and t_s , respectively.

not make any effort to obtain an exact match with observation, but wanted to extract the salient features only.

5. CONCLUDING REMARKS

In this Letter, we presented a simple way to reproduce the HID of outbursting sources from a purely theoretical point of view. We concentrated on the black hole candidates, though a similar approach with an appropriate boundary condition (“hard surface” instead of “absorbing”) would be equally applicable for other compact objects as well.

Our procedure is based on the two-component model (CT95, C97) which has been found to be applicable for both persistent (Chakrabarti & Mandal 2006; Mandal & Chakrabarti 2008) and outburst sources (Chakrabarti et al. 2008, 2009). The major result that arises is that the outbursts may be caused by the sudden enhancement of viscosity which converts a part of the sub-Keplerian accretion rate into the Keplerian accretion rate by angular momentum transport. This was postulated quite some time ago (C97). The reduction of viscosity increases the halo rate back to near normal. Another confirmation of the two-component model is that we found no satisfactory HIDs if both the infall timescales were chosen to be the same or if the shock was absent. The difference in the infall timescales of

the two components and movements of the shock are deciding factors to form the loop structure of the HID. If the shock were absent, there would not be any increase in optical depth and electron temperature for the same amount of injected matter, i.e., the Compton cloud would always be optically thin (C97). In Figure 2, we have shown that by a simple choice of the variation of the two rates one can reproduce the observed diagram quite satisfactorily. It is also clear that the diagram must look different for different objects as the accretion rates, mass of the black hole, duration of the high-viscosity regime, etc. would be different. One may also have to change the definition of the “hardness” from one object to another since what is a hard photon for one black hole could be soft for another. The diagram may look different even for the same object if the accretion rate constants A_f and B_f are different. Furthermore, since the spectral index is highly sensitive in the very high state where the accretion rates are comparable (CT95), there could be fluctuations, especially near region 2, which is observed. This region cannot be reproduced well unless we include detailed time variation of each of these quantities in a very short timescale. One is required to carry out fully time-dependent radiative–hydrodynamic simulations to reproduce such features.

This work is partly supported by the DST Fast Track Young Scientist Project (SR/FTP/PS-21/2006).

REFERENCES

- Chakrabarti, S. K. 1997, *ApJ*, 484, 313
 Chakrabarti, S. K., Debnath, D., Nandi, A., & Pal, P. S. 2008, *A&A*, 489, L41
 Chakrabarti, S. K., Dutta, B., & Pal, P. S. 2009, *MNRAS*, 394, 1463
 Chakrabarti, S. K., & Mandal, S. 2006, *ApJ*, 642, L49
 Chakrabarti, S. K., & Molteni, D. 1995, *MNRAS*, 272, 80
 Chakrabarti, S. K., & Titarchuk, L. G. 1995, *ApJ*, 455, 623
 Choudhury, M., & Rao, A. R. 2004, *ApJ*, 616, L143
 Corbel, S., Tomsick, J. A., & Kaaret, P. 2006, *ApJ*, 636, 971
 Debnath, D., Chakrabarti, S. K., Nandi, A., & Mandal, S. 2008, *Bull. Astron. Soc. India*, 36, 151
 Hjellming, R. M., & Rupen, M. P. 1995, *Nature*, 375, 464
 Mandal, S., & Chakrabarti, S. K. 2008, *ApJ*, 689, L17
 Orosz, J. A., & Bailyn, C. D. 1997, *ApJ*, 477, 876
 Pottschmidt, K., et al. 2006, *A&A*, 452, 285
 Rodriguez, J., Corbel, S., & Tomsick, J. A. 2003, *ApJ*, 595, 1032
 Shakura, N. I., & Sunyaev, R. A. 1973, *A&A*, 24, 337
 Shaposhnikov, N., et al. 2007, *ApJ*, 655, 434
 Smith, D. M., Dawson, D. M., & Swank, J. H. 2007, *ApJ*, 669, 1138
 Smith, D. M., Heindl, W. A., Marketed, C. B., & Swank, J. H. 2001, *ApJ*, 554, 41
 Smith, D. M., Heindl, W. A., & Swank, J. H. 2002, *ApJ*, 569, 362
 Soria, R., Wu, K., Hannikainen, D., McMullough, M., & Hunstead, R. 2001, in *X-ray Emission from Accretion onto Black Holes*, ed. T. Yaqoob & J. H. Krolik, 65 (arXiv:astro-ph/0108084)
 Wu, K., et al. 2002, *ApJ*, 565, 1161